2

Exergy and Environmental Considerations in Gas Turbine Technology and Applications

Richard 'Layi Fagbenle
BSME, PhD (Illinois), MSME(Iowa State), USA

1. Introduction

Global CO_2 emissions by sector in 1990 for transportation, electric power, buildings, synfuels & hydrogen production, and industry were 20%, 27%, 15%, 0% and 38% respectively *[IPIECA Workshop, Baltimore, USA, 12-13 October 2004]*. In a 2095 scenario limiting the GHG to 550 ppm CO_2, the sectoral CO_2 emissions for transportation, electric power, buildings, synfuels & hydrogen production, and industry are 40%, 23%, 19%, 1% and 17% respectively *[IPIECA Workshop, Baltimore, USA, 12-13 October 2004]*. It is argued that the high cost of alternatives, and the strong demand for mobility, limits the effects of climate policies on the transportation sector, while more cost-effective emission reductions are found in the electric power and the industry sectors *[IPIECA Workshop, Baltimore, USA, 12-13 October 2004]*. While it is noted that climate change scenarios are replete with assumptions, the global growth of the transportation sector is undeniable, in both developing and developed countries, as the worldwide passenger travel vs. GDP by region in the figure below for the period 1950-1997 shows *[IPIECA Workshop, Baltimore, USA, 12-13 October 2004]*.

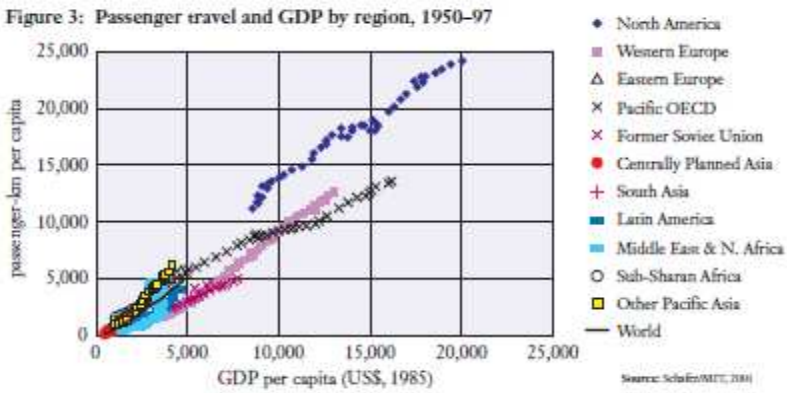

IPIECA Workshop, Baltimore, USA, 12-13 October 2004

In the EU, sectoral CO_2 emissions in 2005 for Energy, Transport, Industry, and Households were 34%, 27%, 21%, and 11%. The Transportation sector breakdown was Road (71.2%), Sea

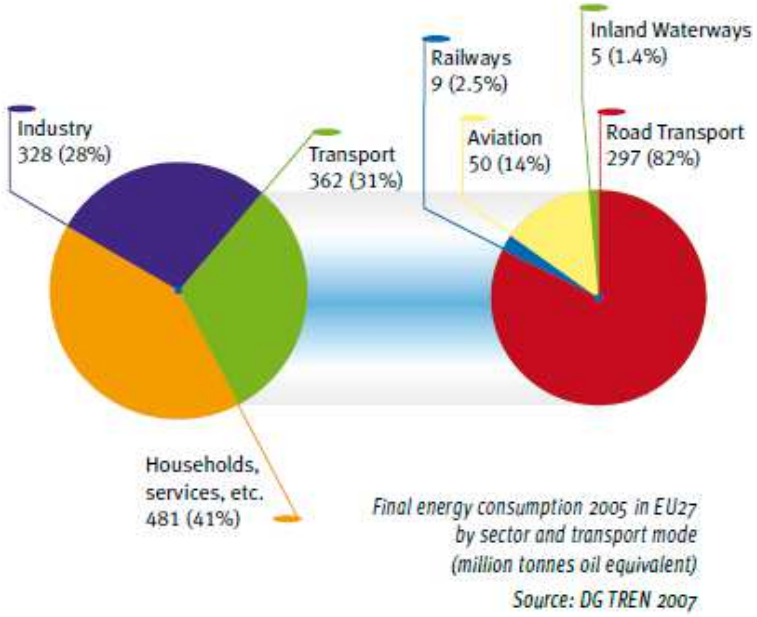

From: Rail Transport and Environment, page 5 – Facts & Figures, Nov. 2008.

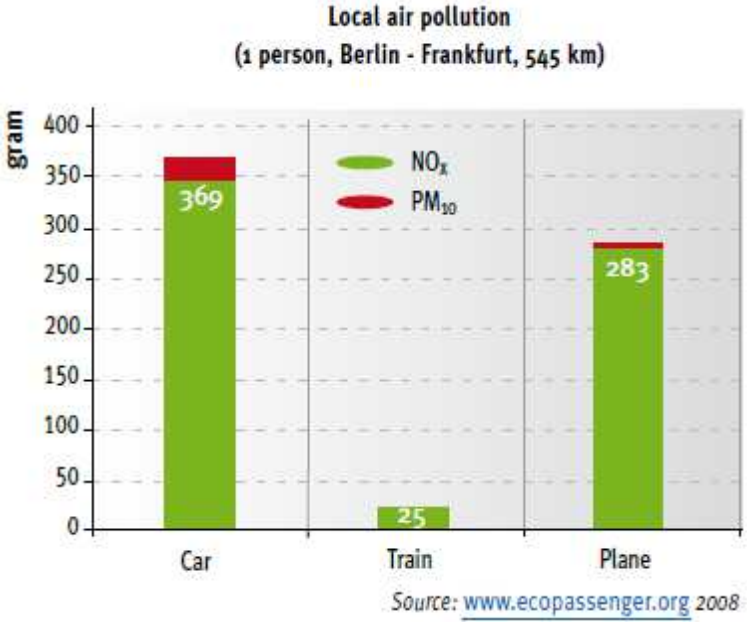

From: Rail Transport and Environment, page 20 – Facts & Figures, Nov. 2008

and Inland Waterways (14.5%), Aviation (11.9%). From: Rail Transport and Environment, page 5 – Facts & Figures, Nov. 2008 *[Rail Transport and Environment, page 5 – Facts & Figures, Nov. 2008]*. The sectoral energy consumption for 2005 appears in the figure shown below, from which the Transportation sector had the second largest share of 31% after the Households & Services sector. Aviation's share of the Transportation sector energy consumption was 14%, second to Road Transport. A similar trend would be found in other regions of the developed world which accounts for the bulk of the global energy consumption and carbon emission.

Similarly, local air pollution data for NO_x and PM_{10} appears below for a journey of 545 km by three modes of transportation.

Transportation of 100 tons of cargo for a distance of 700 km between the Netherlands and Switzerland generates the local pollution information as shown in the figure below:

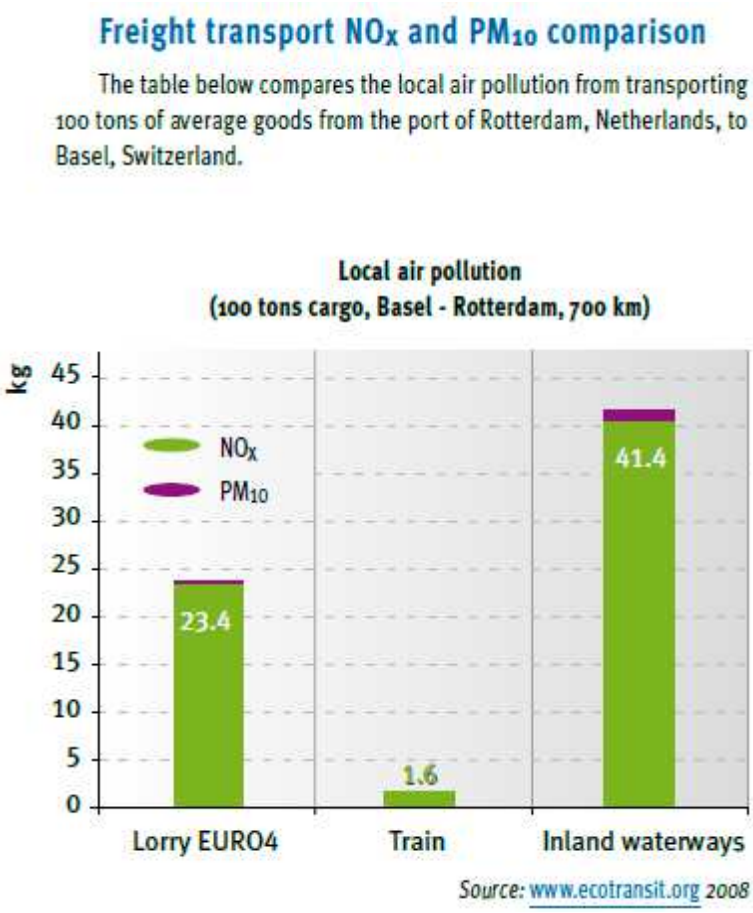

From: Rail Transport and Environment, page 19 – Facts & Figures, Nov. 2008.

Energy efficiency is of utmost importance in addressing the climate problem. Some significant strides have been made by some sub-sectors as the figure below indicates.

In Germany, the consumption of specific energy for Deutsche Bahn, both for regional passenger trains and freight has decreased constantly since 1990, due to the energy efficiency action plan of the company.

Specific primary energy consumption (per pkm or tkm) 1990 - 2007, Deutsche Bahn

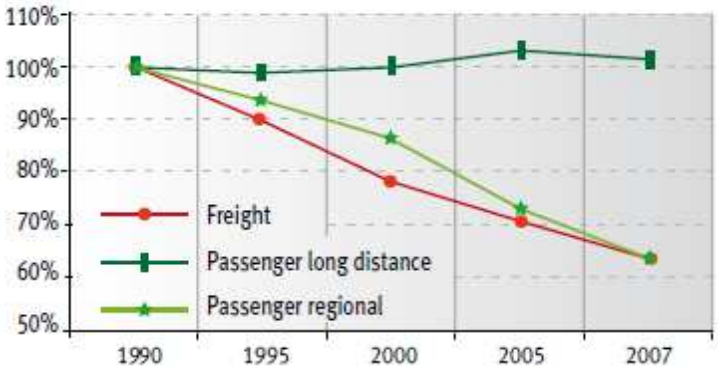

Source: Deutsche Bahn

From: Rail Transport and Environment, page 11 – Facts & Figures, Nov. 2008.

Finally, a look at the noise profile of some modes of transportation is instructive.

Percentages of citizens who are "highly disturbed" when exposed to rail, air and road traffic noise

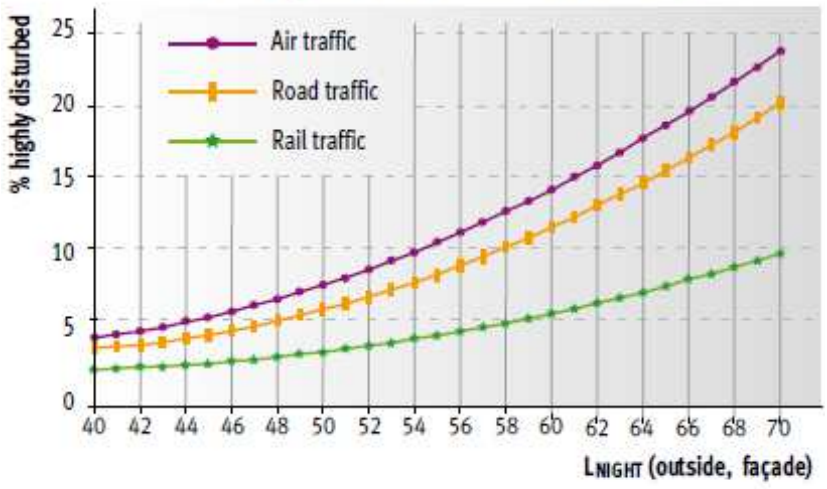

Source: EC 2004

From: Rail Transport and Environment, page 22 – Facts & Figures, Nov. 2008.

From the above, it is clear that just as the other sectors are called upon to reduce their GHG emission, the same should hold for the transportation sector. Gas turbines are employed in the air transportation sub-sector as well as in industry generally. It is claimed that air transport accounts for some 2-3 per cent of all anthropogenic CO2 emissions *[IPIECA Workshop, Baltimore, USA, 12-13 October 2004]*. As of 2004 IPIECA Workshop, there was no substitute envisioned for jet fuel neither was there any niche alternative fuel on the horizon. However, between 2008 and 2010, several test flights have been undertaken with synthetic jet fuel derived from natural gas *[Airline Industry Information, May 3, 2010]* as well as second generation biofuels from 50:50 blend of jathropha oil and standard A1 jet fuel *[The Seattle Times, Dec. 31, 2008]*. Similarly, the Airline Industry Information publication of 16 January 2009 reported that the US Federal Aviation Administration (FAA) has announced the results of a commercial airline test flight using a mixture of jet fuel and biofuel derived from algae and jatropha plants early in January 2009. In June 2009, the aviation fuels subcommittee of the ASTM International was reported to have approved specifications for synthetic aviation fuel, derived from a 50/50 blend of synthetic Fischer-Tropsch fuels and petroleum-derived fuels.

Gas turbines are employed in the Energy, Industrial, and the Transportation Sectors; sectors which have been shown to be responsible for most of the carbon emissions globally. Hence it is imperative to sustain the current drive for improvement in the energy, exergy and environmental performance of gas turbines in general (land, aviation, and marine gas turbine technology). We shall consider some of these issues in this chapter.

2. The Brayton open-cycle components – simple cycle and combined cycle gas turbines

Combustion Chamber/Combustor

Compressed air from the compressor (either centrifugal or axial-flow type) flows directly into the combustion chamber (such as that shown in Fig. 2.1 below) in a Brayton open simple cycle gas turbine where part of it (< 1/3) is used in a direct-fired air heater to burn the fuel after which the remaining air is mixed with the combustion products, all of which is to be carried out with minimum pressure loss. Minimization of pressure is critical at all stages from inlet to the compressor to entry into the turbine to ensure optimal power production from the gas turbine.

The Turbine Chamber of a 3-stage gas turbine plant is shown in Fig. 2.2 and Fig. 2.3 shows a typical turbine stage blades. Substantial volumes of air and combustion gases are moved smoothly and vibration-free through the gas turbine at very high velocities in an axial flow machine, being taken through a series of processes. These processes follow the Brayton cycle processes, viz.: non-isentropic compression from the atmospheric inlet conditions of the compressor to the isobaric (constant-pressure) combustion of the fuel in the combustion chamber, and then followed by adiabatic (non-isentropic) expansion of the hot gases and finally discharging the gases into the atmosphere, all of which is done in a continuous flow process. The energy transfer between the fluid and the rotor in the compression and expansion processes is achieved by means of kinetic action rather than by positive displacement as occurs as in reciprocating machines.

Fig. 2.1. A Combustion Chamber Can. [From Shepherd, D.G., Introduction to the Gas Turbine, D. Van Nostrand Co., Inc.

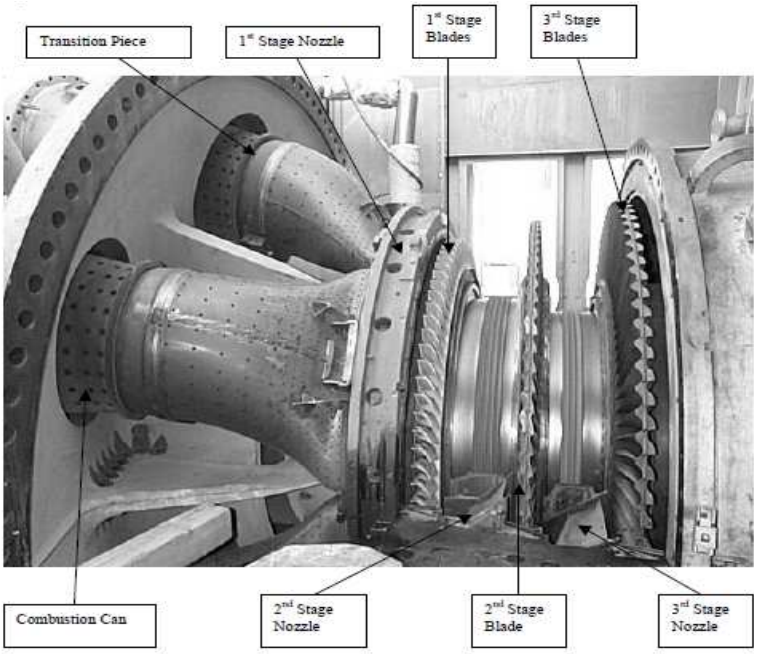

Fig. 2.2. The Turbine Chamber of a 3-stage turbine plant. [From Shepherd, D.G., Introduction to the Gas Turbine, D. Van Nostrand Co., Inc.

Fig. 3.3. Typical turbine stage. [From Shepherd, D.G., Introduction to the Gas Turbine, D. Van Nostrand Co., Inc.

4. Gas turbine fuels – conventional and new fuels

Conventional gas turbine fuels currently in use are exclusively liquid and gaseous and usually hydrocarbons. Solid gas turbine fuel technology is still in the research and developmental stages. New gas turbine fuels, as mentioned earlier in the Introduction, include the synthetic Fischer-Tropsch aviation jet fuels and the second generation biofuels.

Conventional gas turbine fuels – Liquid and gaseous fuels

Conventional gas turbine liquid fuels include the range of refined petroleum oils from highly refined gasoline through kerosene and light diesel oil to a heavy residual oil (Bunker C or No. 6 fuel oil). Table 4-1 gives the ultimate analysis of some liquid fuels.

Fuel	Carbon	Hydrogen	Sulfur	Ash, etc.
100 Octane petrol	85.1	14.9	0.01	-
Motor petrol	85.5	14.4	0.1	-
Benzole	91.7	8.0	0.3	-
Kerosene (paraffin)	86.3	13.6	0.1	-
Diesel oil	86.3	12.8	0.9	-
Light fuel oil	86.2	12.4	1.4	-
Heavy fuel oil	86.1	11.8	2.1	-
Residual fuel oil	88.3	9.5	1.2	1.0

Table 4.1. Ultimate analysis of some liquid fuels. (From Applied Thermodynamics for Engineering Technologists, S.I. Units by Eastop & McConkey, 2nd ed., 1970).

Table 4-2 below also indicates some of the key properties of some of the many known hydrocarbons.

Team, Air, and Gas PowerFamily Name	Formu - la	Melting Temp., °C	Boiling Temp., °C	SIT++ °C	Specific Gravity	API Gravity	HHV kJ/kg	LHV kJ/kg	Mixture kJ/m³	Latent Heat, kJ/kg	Octane Rating	Performance No. (4 ml TEL/gal.) Lean[a]	Rich	Mol. Wt.
1. Gas C_nH_{2n+2} Methane	CH_4	-182.2	-161.1	730	0.424	202.5	55,475	50,235	3241.5	576.85	110[a]	……	……	16.0
2. Gas C_nH_{2n+2} Ethane	C_2H_6	-172.2	-88.3	566	0.546	194.0	52,102	47,909	3439.0	407.05	104[a]	……	……	30.0
3. LPG C_nH_{2n+2n} Propane	C_3H_8	-186.7	-42.2	535	0.582	142.0	50,358	46,555	3491.2	388.44	100	……	……	44.0
4. LPG C_nH_{2n+2n} Butane	C_4H_{10}	-135	-0.56	516	0.570	116.5	49,544	46,043	3532.1	383.79	92	……	……	58.1
5. LPG C_nH_{2n+2n} Pentane	C_5H_{12}	-129.4	36.1	501	0.626	94.5	49,079	45,583	3550.8	374.49	61	63	63	72.1
6. Gasoline C_nH_{2n+2n} n-Heptane	C_7H_{16}	-90.6	98.9	478	0.684	75.5	48,497	45,143	3591.8	307.03	0	0[b]	0[b]	100.2
7. Gasoline C_nH_{2n+2n} Triptane	C_7H_{16}	-25	81.1	……	0.690	……..	……	44,427	……	290.75	…….	200	360	100.2
8. Gasoline C_nH_{2n+2n} Iso-Octane	C_8H_{18}	-107.8	99.4	732	0.692	73.5	47,869	44,564	3558.2	297.73	100	153	153	114.2
9. Fuel Oil C_nH_{2n+2} Decane	$C_{10}H_{22}$	-30	173.9	463	0.730	62.5	47,916	44,671	3599.2	251.21	……..	……	……	142.3
10. Fuel Oil C_nH_{2n+2n} Dodecane	$C_{12}H_{26}$	-10	216.1	……	0.749	57.5	47,799	44,596	3610.4	248.88	……..	……	……	170.3
11. Fuel Oil C_nH_{2n+2n} Hexadecane	$C_{16}H_{34}$	18.3	280	……	0.774	51.5	47,497	44,348	3610.4	……	100	……	……	226.4
12. Fuel Oil C_nH_{2n+2n} Octadecane	$C_{18}H_{38}$	27.8	307.8	……	0.782	49.5	47,450	44,303	3625.3	…….	……	……	……	245.5
13. Olefins C_nH_{2n} Propene	C_3H_6	-185	-47.8	……	0.61	103.0	48,846	45,241	3595.5	…….	85	……	……	42.1
14. Olefins C_nH_{2n} Butene-1	C_4H_8	-195	-6.7	……	0.625	……	48,613	45,008	3614.1	……..	82	84	……	56.1
15. Olefins C_nH_{2n} Hexene-1	C_6H_{12}	-137.8	63.3	……	0.675	76.0	44,310	41,317	3576.9	388.44	84.1	……	……	84.1
16. Napthenes C_nH_{2n} Cyclopentane	C_5H_{10}	-94.4	49.4	……	0.746	56.7	43,682	40,691	3506.1	……..	82	100	>160	70.1
17. Naphthenes C_nH_{2n} Cyclohexane	C_6H_{12}	6.7	80.6	……	0.778	51.6	43,519	40,547	3506.1	362.86	77	84	130	84.1
18. Aromatics C_nH_{2n-6} Benzene	C_6H_6	5.6	80.6	739	0.88	29.0	42,240	39,984	3606.7	393.09	110[a]	68	>160	78.1
19. Aromatics C_nH_{2n-6} Toluene	C_7H_8	-95	110.6	811	0.87	31.0	42,566	40,612	3688.6	362.86	104[a]	95	>160	92.1
20. Aromatics C_nH_{2n-6} Xylene	C_8H_{10}	-26.1	140.6	……	0.86	31.0	43,031	40,705	3632.7	337.27	105[a]	……	……	106.2
21. Alcohols Methanol	CH_3OH	-97.8	65	……	0.792	46.4	22,725	20,106	3353.3	1167.65	98	<75	>180	32.0
22. Alcohols Ethanol	C_2H_6O	-117.2	77.8	……	0.785	47.1	29,726	26,991	3494.9	921.10	99	<75	>180	46.0
23. Tetraethyl lead	$C_8H_{20}Pb$	-136.1	182.2	……	1.653	……	…….	…….	……	169.80	……	……	……	……..
24. Hydrogen (gas)	H_2	……	……	……	……	……	…….	10,002	……	……	……	……	……	2.0
25. Water	H_2O	0	100	……	0.998	……	…….	0	……	2256.22	……	……	……	18.0
26. Carbon (solid)	C	…….	……	……	……	……	…….	32,564	……	……	……	……	……	12.0
27. Gasoline (straight run)	……..	-60	43-149	……	……	……	……	44,194	……	……	140[a]	78	93	……..
28. Carbon monoxide	CO	……	-191.7	609	……	……	10,111	10,111	……	……	……	……	……	28.0

Table 4.2. Abstracted from Table V Properties of Hydrocarbons of Steam, Air & Gas Power by Severns, Degler & Miles, John Wiley, 5th ed. 1964. S.I. Units conversion done by Prof. Richard Fagbenle. SIT – Self-ignition temperature;

Fig. 4-1 below shows typical distillation characteristics for military and commercial aircraft fuels. Relative to the "pure substance" single evaporation temperatures of water and ethyl alcohol, gasoline is a mixture of liquid several hydrocarbons and its various components boil off at different temperatures as can be seen in the graphs.

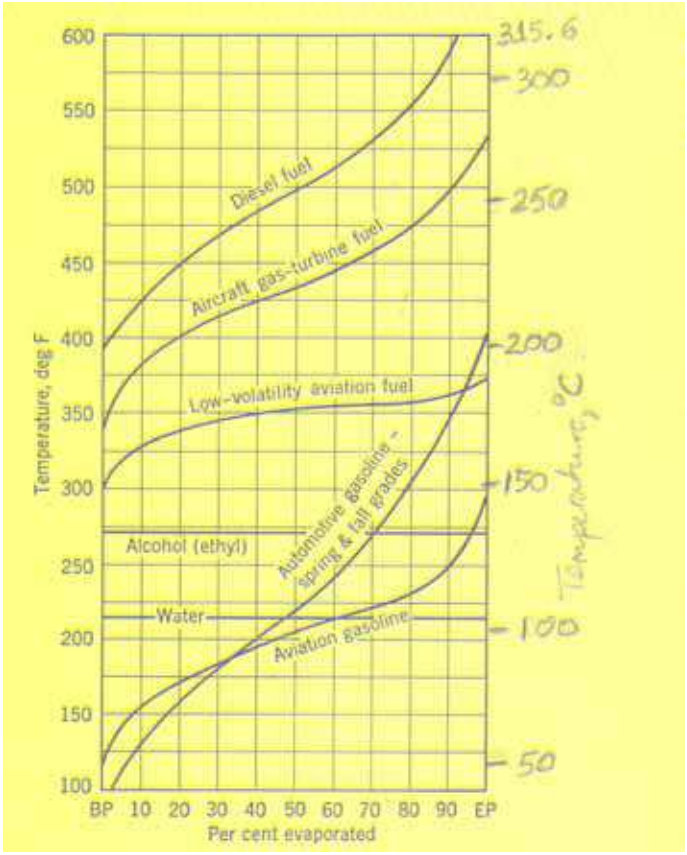

Fig. 4.1. Typical ASTM distillation characteristics for various types of fuels. Degree Centigrade scale supplied by Prof. R. 'Layi Fagbenle. Abstracted from Steam, Air, and Gas Power by Severns, Degler & Miles, John Wiley & Sons Inc. 1964.

The aviation gasoline graph at the bottom of the graph is for piston-engine powered aircraft and it has a low flash point to improve its ignition characteristics. It is usually a high-octane gasoline known as "avgas". Turbine engines on the other hand can operate with a wide range of fuels, but typically use fuels with much higher flash points, less flammable and generally safer to store and transport. Most jet fuels are basically kerosene-based. Both the Jet A specification fuel used in the USA and the Jet A-1 standard specification of most of the rest of the world have a relatively high flash point of 38°C and a self-ignition temperature (SIT) (or auto-ignition temperature) of 210°C, making them safer to handle than the traditional avgas. The open air burning temperature in Table 4-2 can be compared with the typical distillation characteristics for aircraft gas turbine fuel in Fig. 4-1.

Physical Properties	Jet A-1	Jet A
Flash Point	> 38°C (100.4 °F)	
Self- (auto-) ignition temperature	210 °C (410 °F)	
Freezing point	< -47 °C (-52.6 °F)	< -40 °C (-40 °F)
Open air burning temperature	287.5 °C (549.5 °F)	
Density (per litre)	0.775 kg/l – 0.840 kg/l	
Specific energy (calorific value)	> 42.80 MJ/kg	

Table 4.2. Typical Specifications for Jet A and Jet A-1 Aircraft Fuels (from Wikipedia)

Specifications for Heavy-Duty Gas Turbine Fuels

Heavy-duty gas turbines are able to burn a wide range of gaseous fuels and hence are less restricted in their fuel classifications. A typical heavy-duty gas turbine fuel specification (range only indicated) appears in Table 4-3 below.

Fuel	LHV [MJ/m^3]	Major Components
Natural Gas and Liquefied Natural Gas (LNG)	29.81 – 7.45	Methane
Liquefied Petroleum Gas [LPG]	85.70 – 119.23	Propane; Butane
Gasification Gases (Air Blown)	3.73 – 5.50	CO; H_2; N; H_20_v
Gasification Gases (Oxygen Blown)	7.45 – 14.90	CO; H_2; H_20_v
Process Gases	11.20 – 37.30	CH_4; H_2; CO; CO_2

Table 4.3. Range of typical heavy-duty gas turbine fuel classification (adapted from GEI 41040G – GE Gas Power Systems, Revised January 2002).

The feedstock for gasification fuels can be coal, petroleum coke or heavy liquids. Gasification fuels generally have lower much lower heating values than other fuel gases, and they are produced by one of two processes: oxygen blown or air blown gasification process.

Process gases are generated by many petrochemical and chemical processes and are suitable for fuelling gas turbines, for example refinery gases). Constituents of process gases include CH_4, H_2, CO, and CO_2. Other process gases used as gas turbine fuels are byproducts of steel production such as blast furnace gases and coke oven gases. Blast Furnace Gases (BFG) have heating values below minimal allowable limits for gas turbine fuels, necessitating blending with other fuels such as coke oven gas, natural gas or hydrocarbons such as propane or butane.

Typical gas turbine fuel specification ranges appear in Table 4-4 below. In addition to such specifications which may be particular to each turbine manufacturer, allowable gas fuel contaminant levels are also specified for such trace metals as (Pb, V, Ca, and Mg), Alkali metals (Na and K) and particulates. Sodium (Na) is the only trace metal contaminant normally found in natural gas, and it source is salt water in the ground gas wells.

Sources of contaminants in heavy-duty gas turbine applications include particulates arising largely from corrosion chemical reactions in gas pipelines, liquid (water and/or hydrocarbon) condensates and lubricating oils from compressor stations; sulfur (as H_2S or COS); trace metals; steam and water for injection; alkali metals contained in compressor discharge; and the fuel.

Fuel Properties	Max	Min	Notes
Lower Heating Value, MJ/m^3	None	3.73 –11.20	
Modified Wobbe Index (MWI) - Absolute limits - Range within limits	54 +5%	40 -5%	
Flammability Ratio		2.2:1	Rich:Lean Fuel/Air Ratio, volume basis
Constituent Limits, mole %			
Methane, CH_4	100	85	% of reactant species
Ethane, C_2H_6	15	0	% of reactant species
Propane, C_3H_8	15	0	% of reactant species
Butane C_4H_{10} + higher	5	0	% of reactant species
paraffins (C_4+)	Trace	0	% of reactant species
Hydrogen, H_2	Trace	0	% of reactant species
Carbon monoxide, CO	Trace	0	% of reactant species
Oxygen, O_2	Trace	0	% of reactant species
Total Inerts (N_2+CO_2+Ar)	15	0	% of total (reactants + inerts)
Aromatics (Benzene C_6H_6,			
Toluene C_7H_8, etc.)	Report	0	
Sulfur	Report	0	

Table 4.4. Range of typical heavy-duty gas turbine fuel specification (adapted from GER 41040G – GE Gas Power Systems, Revised January 2002).

Conventional and New Environmental-conscious Aero and Industrial Gas Turbine Fuels

Conventional aero gas turbine fuels are commonly:

i. Kerosene from crude petroleum sources using established refining processes, and
ii. synthetic kerosene from Fischer-Tropsch (FT) synthesis using coal, natural gas, or any other hydrocarbon feedstock (e.g. shale, tar sands, etc.). These are produced by first gasifying the hydrocarbon resource followed by liquefaction to form hydrocarbon liquids (e.g. as earlier noted, the Airline Industry Information update dateline 26 June 2009)

New Environmentally-conscious aero gas turbine fuels are:

i. Bio-fuels from bio-derived Fatty Acid Methyl Esters (FAME) mixed with conventional aero fuel (kerosene) in regulated proportions,
ii. Bio-ethanol and bio-methanol neat or mixed in regulated proportions with gasoline,
iii. Biofuels produced from Fischer-Tropsch Synthesis (FTS) process using biomass feedstock such as oil seeds – jathropha, palm oil, soybeans, rapeseed (canola), sunflower, camelina, etc., as well as animal fats,
iv. Bio-syngas produced by gasification of biomass, lignocellulosic biomass and other agricultural wastes used as feed into the FTS (2nd generation biofuels) to produce liquid fuels (FTL), and
v. Liquefied petroleum gas (LPG) which is really not a cryogen; Liquefied gases such as LNG, Methane and Hydrogen. Both methane and hydrogen will have to be liquefied for use as aircraft fuel.

Table 4.5 below gives relative properties of conventional aviation kerosene and typical biodiesel aircraft fuel (will vary with Fatty Acid Methyl Esters [FAME] type):

Property	Aviation Kerosene	Bio-diesel	20% Blend	Impact
Heat of combustion [MJ/kg] typical	43.2	32 – 39	41.0 – 42.4 (spec. min: 42.8)	Airframe range/loading
Density [kg/m^3] range	775 – 840	860 – 900	792 – 852	
Viscosity [mm2/sec @ -20°C max.				Wing tank temp. limits, Cold Starts & Relight.
Approx. Carbon length	C14 – C15 max (trace levels)	C16 – C22	C16 – C22	Combustion emissions
Flash point, °C min.	38	>101	Unchanged	
Freeze Point,°C max	-47	-3? 0	-5 to -10 with additives	Wing tank temp. limits, Cold Start and Relight.
Sulfur [ppm] max	3000	10		
Acidity [mg KOH/g] max	0.015	0.5	0.11	Material compatibility
Phosphorous [ppm] max	Excluded	10	2	Hot-end life
Metals [ppm] max	Excluded	5	1	Hot-end life
Thermal Stability	Controlled to well defined level	Not controlled	Not known	Fuel system & injector life
Composition	Hydrocarbon	FAME	20% FAME	Elastomer compatibility

From: Ppt. Presentation by Chris Lewis, Company Specialist – Fluids, Rolls Royce plc, titled "A Gas Turbine Manufacturer's View of Biofuels". 2006.

In the steam-reforming reaction, steam reacts with feedstock (hydrocarbons, biomass, municipal organic waste, waste oil, sewage sludge, paper mill sludge, black liquor, refuse-derived fuel, agricultural biomass wastes and lignocellulosic plants) to produce bio-syngas. It is a gas rich in carbon monoxide and hydrogen with typical composition shown in Table 4.6 below.

Constituents	% by vol. (dry & N_2-free)
Carbon monoxide (CO)	28 – 36
Hydrogen (H_2)	22 – 32
Carbon dioxide (CO_2)	21 – 30
Methane (CH_4)	8 – 11
Ethene (C_2H_4)	2 – 4
Benzene-Toluene-Xylene (BTX)	0.84 – 0.96
Ethane (C_2H_5)	0.16 – 0.22
Tar	0.15 – 0.24
Others (NH3, H2S, HCl, dust, ash, etc.)	< 0.021

Source: M. Balat et al. Energy Conversion and Management 50 (2009) 3158 – 3168).

Table 4.6. Typical composition of bio-syngas from biomass gasification.

A useful reference for the thermo-conversion of biomass into fuels and chemicals can be found in the above referenced paper by M. Balat et al.

Ethanol-powered gas turbines for electricity generation

In a 2008 report by Xavier Navarro (RSS feed), a company called LPP Combustion (Lean, Premixed, Prevaporized) was claimed to have demonstrated that during gas turbine testing, emissions of NOx, CO, SO_2 and PM (soot) from biofuel ethanol (ASTM D-4806) were the same as natural gas-level emissions achieved using dry low emission (DLE) gas turbine technology. It was also claimed that the combustion of the bio-derived ethanol produced virtually no net CO_2 emissions.

Gas Turbines and Biodiesels

A recent study by Bolszo and McDonnell (2009)[1] on emissions optimization of a biodiesel-fired 30-kW gas turbine indicates that biodiesel fluid properties result in inferior atomization and longer evaporation times compared to hydrocarbon diesel. It was found that the minimum NOx emission levels achieved for biodiesel exceeded the minimum attained for diesel, and that optimizing the fuel injection process will improve the biodiesel NOx emissions.

A theoretical study was recently carried out by Glaude et al. (2009)[2] to clarify the NOx index of biodiesels in gas turbines taking conventional petroleum gasoils and natural gas as reference fuels. The adiabatic flame temperature T_f was considered as the major determinant of NOx emissions in gas turbines and used as a criterion for NOx emission. The study was necessitated by the conflicting results from a lab test on a microturbine and two recent gas turbine field tests, one carried out in Europe on rapeseed methyl ester (RME) and the other in USA on soybean methyl ester (SME), the lab test showing a higher NOx emission while the two field tests showed slightly lower NOx emission relative to petroleum diesel. It is however clear that biodiesels have reduced carbon-containing emissions and there is agreement also on experimental data from diesel engines which indicate a slight increase in NOx relative to petroleum diesel. The five FAME's studied by Glaude et al. were RME, SME, and methyl esters from sunflower, palm and tallow.

The results showed that petroleum diesel fuels tend to generate the highest temperatures while natural gas has the lowest, with biodiesel lying in-between. This ranking thus agrees with the two field tests mentioned earlier. It was also found out that the variability of the composition of petroleum diesel fuels can substantially affect the adiabatic flame temperature, while biofuels are less sensitive to composition variations.

5. Factors limiting gas turbine performance

The Joule cycle (also popularly known as the Brayton cycle) is the ideal gas turbine cycle against which the performance (i.e. the thermal efficiency of the cycle η_{CY}) of an actual gas turbine cycle is judged under comparable conditions. We prefer to restrict the use of Joule

[1] C. D. Bolszo and V. G. McDonell, Emissions optimization of a biodiesel fired gas turbine, Proceedings of the Combustion Institute, Vol 32, Issue 2, 2009, Pages 2949-2956.

[2] Pierre A. Glaude, Rene Fournet, Roda Bounaceur and Michel Moliere, (2009). Gas Turbines and Biodiesel: A clarification of the relative NOx indices of FAME, Gasoil and Natural Gas.

cycle to the ideal gas turbine cycle while the Brayton cycle is exclusively used for the actual gas turbine cycle. The ideal gas turbine "closed"cycle (or Joule cycle) consists of four ideal processes – two isentropic and two isobaric processes – which appear as shown in Fig. 5.1. The thermal efficiency of the Joule cycle in terms of the pressure ratio r_p given by $r_p = \frac{p_B}{p_A}$ and the pressure ratio parameter ρ_p given by $\rho_p = r_p^{(\gamma-1)/\gamma}$ is:

$$\eta_{\text{Joule}} = \left(1 - \frac{1}{r_p^{(\gamma-1)/\gamma}}\right) = \left(1 - \frac{1}{\rho_p}\right) \tag{5.1}$$

Hence, the thermal efficiency of the ideal gas Joule cycle is a function only of the pressure ratio. Since for isentropic processes 1-2 and 3-4, $\frac{T_2}{T_1} = \frac{T_3}{T_4} = \rho_p$, the Joule efficiency is also dependent of the isentropic temperature ratios only, but independent of the compressor and the turbine inlet temperatures separately without a knowledge of the pressure ratio. Thus, ρ_p is essentially the isentropic temperature ratio, the abscissa in Fig. 5.1. If air is the working fluid employed in the ideal Joule cycle, the cycle is referred to as the air-standard Joule cycle.

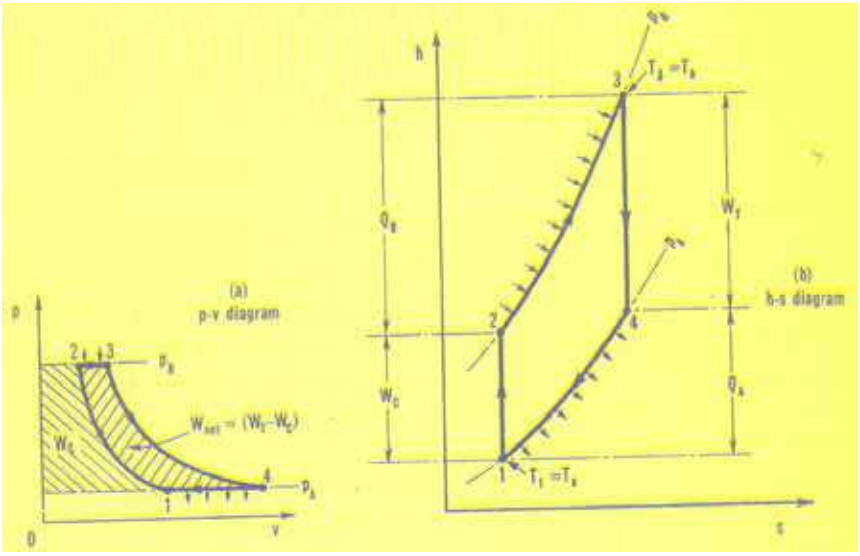

Fig. 5.1. Ideal Joule cycle (a) p-V and (b) T-s state diagrams. From Haywood [ ].

Fixing the inlet temperature to the compressor T_a and the inlet temperature to the turbine T_b automatically sets a limit to the pressure ratio r_p, which occurs when the temperature after isentropic compression from T_a is equal to the TIT T_b. However, when this occurs, the net work done is seen to be equal to zero, as the area of the cycle on the T-s and p-V diagrams indicate.

Haywood considers an interesting graphical representation of eq. 5.1 above for T_a = 15°C and T_b = 100°C as shown in Fig. 5.2

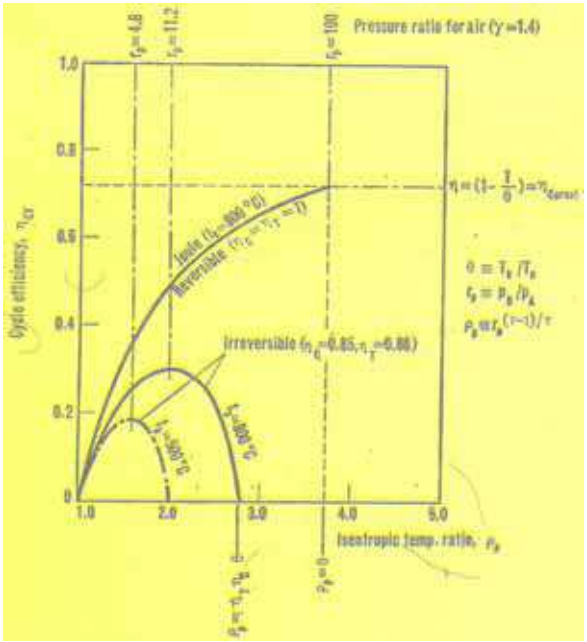

For T_a = 15°C and T_b = 100°C, η_{Joule} increases continuously with rp right up to the limiting value as the curve labeled "reversible" shows. The limiting pressure ratio r_p = 99.82 approximated to 100 in the figure is attained when $\rho_p = \theta = T_b/T_a = 1073/288 = 3.7257$. Under this condition, a sketch of the Joule cycle on the T-s diagram shows that as r_p approaches this value, the area enclosed by the cycle approaches zero. However, In practical terms, a pressure ratio this large is never used when issues of process irreversiblities are considered, to which the remaining two curves in the graph pertain.

Fig. 5.2. Variation of cycle efficiency with Isentropic temperature ratio ρ_p (t_a = 15°C). From Haywood [ ].

5.1 Effect of irreversibilities in the actual gas turbine cycle

In an actual plant, frictional effects in turbines and compressors and pressure drops in heat exchangers and ductings and combustion chamber are basically lost opportunities for production of useful work. The h-s curve diagram for such a gas turbine Brayton cycle appears in Fig. 5.3, wherein the heat and work terms in each of the processes are identified, ignoring the frictional effects in the heat exchangers, ductings and combustion chamber. We note that the compressor work input required W_C, is now much larger than its previous value for the ideal Joule cycle while the turbine work output W_T is considerably smaller than for the ideal Joule cycle, revealing the considerable effect of turbine and compressor inefficiencies on the cycle thermal efficiency. An analytic expression for the Brayton cycle thermal efficiency can be shown to be:

$$\eta_{Brayton} = \frac{(1 - 1/\rho_p)(\alpha - \rho_p)}{(\beta - \rho_p)} \tag{5.2}$$

where $\alpha = \eta_C\eta_T\theta$, $\beta = [1 + \eta_C(\theta - 1)]$, and $\theta = T_b/T_a$.

In Fig. 5.2, the actual Brayton cycle performance is depicted for turbine and compressor isentropic efficiencies of 88% and 85% respectively, t_a = 15°C for two values of t_b = 800°C and 500°C respectively. The optimum pressure ratio is now reduced from approximately 100 to 11.2 for t_b = 800°C, and to only 4.8 at t_b = 500°C. This optimum pressure ratio is more realistically achievable in a single compressor. Here also, we find that $\eta_{Brayton}$ is highly dependent on $\theta = T_b/T_a$, showing a drastic reduction from TIT = 800°C to TIT = 500°C.

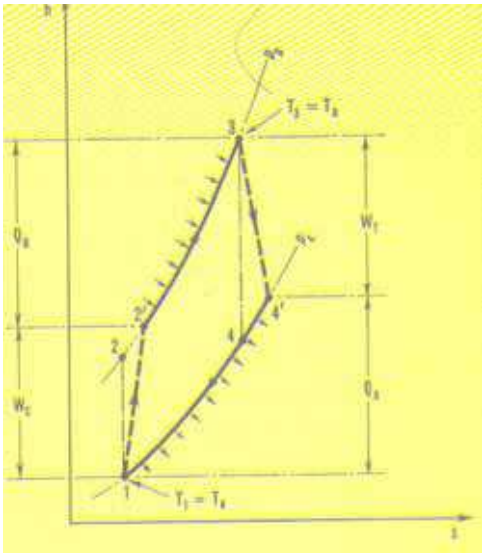

The compressor work input per unit mass of working fluid is

$$W_c = c_p(T_{2'} - T_a) = \frac{c_p T_a}{\eta_c}(\rho_p - 1) \qquad (5.3)$$

while

$$W_T = c_p(T_b - T_4') = c_p \eta_T T_b \left(1 - \frac{1}{\rho_p}\right) \qquad (5.4)$$

and

$$W_{net} = (W_T - W_C) = \frac{c_p T_a}{\eta_c}\left(1 - \frac{1}{\rho_p}\right)(\alpha - \rho_p) \qquad (5.5)$$

with $\alpha = \eta_C \eta_T \theta$ and $\theta = T_b/T_a$ as before.
From 5.5, W_{net} vanishes when $\rho_p = 1$ and when $\rho_p = \alpha$. Also from differentiating 5.5 w.r.t. ρ_p, we obtain that W_{net} is maximum when $\rho_p = \sqrt{\alpha}$. The variation of W_{net} with the adiabatic temperature ratio ρ_p appears in Fig. 5.4.

Fig. 5.3. Enthalpy-entropy diagram for Actual Brayton cycle, with turbine and Compressor inefficiencies. From Haywood [ ].

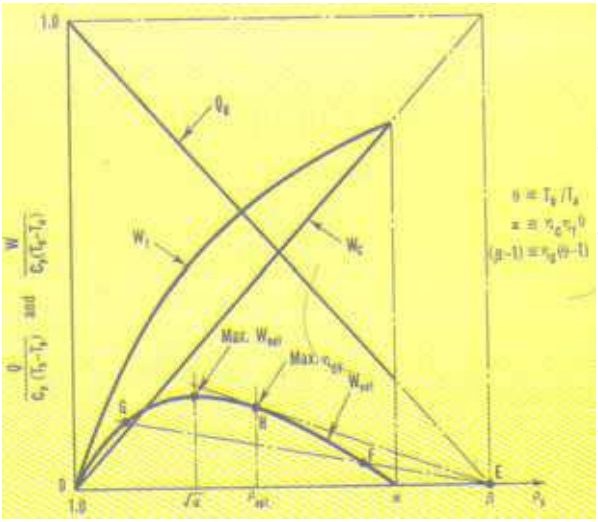

Haywood [] discusses the graphical construction in Fig. 5.4 due to Hawthorne and Davis [ ] for the variation of Q_B, W_T, W_C, and W_{net} with variation in ρ_p for fixed values of T_a and T_b. The maximum efficiency is obtained at the value of ρ_p corresponding to the point H at which a straight line from point E is tangent to the curve for W_{net}, i.e at $\rho_p = \rho_{opt}$. The method indicates that the points of maximum thermal efficiency of the Brayton cycle η_{CY} and the maximum W_{net} are not coincident; rather the value of ρ_p is greater for the former than for the latter. It may also be shown that, if ρ_W and ρ_{opt} are the values of ρ_p for maximum W_{net} and maximum η_{CY} respectively, then $\frac{\rho_w}{\rho_{opt}} = \sqrt{(1-\eta_m)}$ where η_m is the maximum value of the thermal efficiency of the Brayton cycle.

Fig. 5.4. Variation of heat supplied to the combustor Q_B, turbine work output W_T, compressor work input W_C, and W_{net} with isentropic temperature ratio ρ_p. From Haywood [ ].

Figs. 5.5 and 5.6 show the schematic of the simple-cycle, open-flow gas turbine with a single shaft and double shaft respectively. The single shaft units are typically used in applications requiring relatively uniform speed such as generator drives while in the dual shaft applications, the power turbine rotor is mechanically separate from the high-pressure turbine and compressor rotor. It is thus aerodynamically coupled, making it suitable for variable speeds applications.

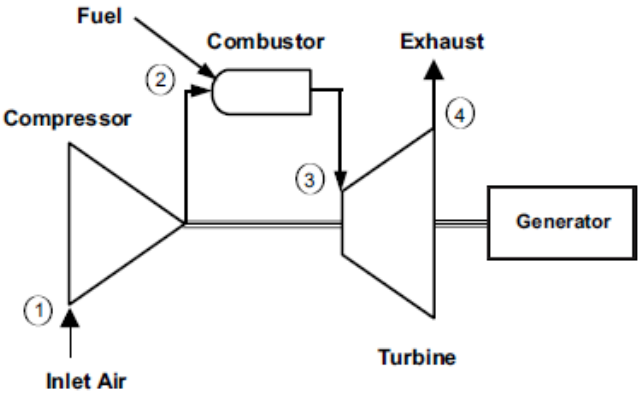

Fig. 5.5. Simple-cycle, open-flow, single-shaft gas turbine

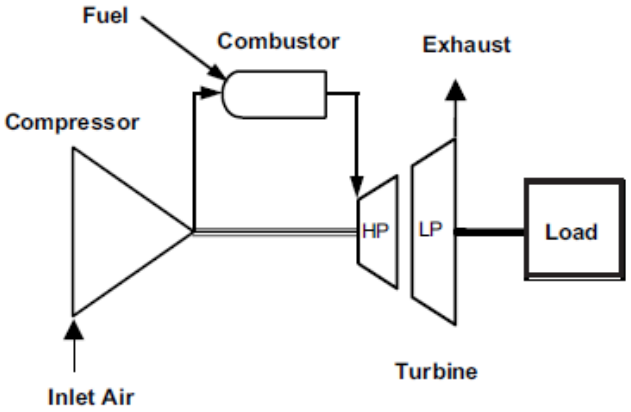

Fig. 5.6. Simple cycle, open-flow, dual-shaft gas turbine for mechanical drives.

5.2 Simple-cycle vs. Combined-cycle gas turbine power plant characteristics

Fig. 5.7 shows the variation of output per unit mass and efficiency for different firing temperatures and pressure ratios for both simple-cycle and combined-cycle applications. In the simple-cycle top figure, at a given firing temperature, an increase in pressure ratio results in significant gains in thermal efficiency. The pressure ratio resulting in maximum efficiency and maximum output are a function of the firing temperature; the higher the pressure ratio, the greater the benefits from increased firing temperature. At a given